Hydroxyl Ethyl Starch (HES) Preserves Intrarenal Microcirculatory Perfusion Shown by Contrast-Enhanced Ultrasound (Ceus), and Renal Function in a Severe Hemodilution Model in Pigs

Ergin, Bülent; van Rooij, Tom; Lima, Alexandre; Ince, Yasin; Specht, Patricia A.C.; Mik, Egbert G.; Kooiman, Klazina; de Jong, Nico; Ince, Can

DOI
10.1097/SHK.0000000000001862

Publication date
2022

Document Version
Final published version

Published in
Shock (Augusta, Ga.)

SHOCK, Vol. 57, No. 3, pp. 457–466, 2022

HYDROXYL ETHYL STARCH (HES) PRESERVES INTRARENAL MICROCIRCULATORY PERFUSION SHOWN BY CONTRAST-ENHANCED ULTRASOUND (CEUS), AND RENAL FUNCTION IN A SEVERE HEMODILUTION MODEL IN PIGS

Bülent Ergin,[*] Tom van Rooij,[†] Alexandre Lima,[*] Yasin Ince,[*] Patricia A.C. Specht,[‡] Egbert G. Mik,[‡] Klazina Kooiman,[†] Nico de Jong,[†§] and Can Ince[*]

[*]Department of Intensive Care, Laboratory of Translational Intensive Care, Erasmus MC, University Medical Center Rotterdam, Rotterdam, The Netherlands; [†]Department of Biomedical Engineering, Thorax Center, Erasmus MC, Rotterdam, The Netherlands; [‡]Laboratory of Experimental Anesthesiology, Department of Anesthesiology, Erasmus MC, Rotterdam, The Netherlands; and [§]Laboratory of Acoustical Wavefield Imaging, Department of Applied Sciences, Delft University of Technology, Delft, The Netherlands

Received 15 Jun 2021; first review completed 9 Jul 2021; accepted in final form 9 Sep 2021

ABSTRACT—Acute normovolemic hemodilution (ANH) is associated with low oxygen carrying capacity of blood and purposed to cause renal injury in perioperative setting. It is best accomplished in a perioperative setting by a colloid such as hydroxyl ethyl starch (HES) due its capacity to fill the vascular compartment and maintain colloidal pressure. However, alterations of intra renal microvascular perfusion, flow and its effects on renal function and damage during ANH has not been sufficiently clarified. Based on the extensive use of HES in the perioperative setting we tested the hypothesis that the use of HES during ANH is able to perfuse the kidney microcirculation adequately without causing renal dysfunction and injury in pigs. Hemodilution (n = 8) was performed by stepwise replacing blood with HES to hematocrit (Hct) levels of 20% (T1), 15% (T2), and 10% (T3). Seven control animals were investigated. Systemic and renal hemodynamics were monitored. Renal microcirculatory perfusion was visualized and quantified using contrast-enhanced ultrasound (CEUS) and laser speckle imaging (LSI). In addition, sublingual microcirculation was measured by handheld vital microscopy (HVM). Intrarenal mean transit time of ultrasound contrast agent (IRMTT-CEUS) was reduced in the renal cortex at Hct 10% in comparison to control at T3 (1.4 ± 0.6 vs. 2.2 ± 0.7 seconds, respectively, $P < 0.05$). Although renal function was preserved, the serum neutrophil gelatinase-associated lipocalin (NGAL) levels was higher at Hct 10% (0.033 ± 0.004 pg/μg protein) in comparison to control at T3 (0.021 ± 0.002 pg/μg protein. A mild correlation between CO and IRMTT (renal RBC velocity) (r −0.53; $P = 0.001$) and CO and NGAL levels (r 0.66; $P = 0.001$) was also found. Our results show that HES induced ANH is associated with a preserved intra renal blood volume, perfusion, and function in the clinical range of Hct (<15%). However, at severely low Hct (10%) ANH was associated with renal injury as indicated by increased NGAL levels. Changes in renal microcirculatory flow (CEUS and LSI) followed those seen in the sublingual microcirculation measured with HVM.

KEYWORDS—Acute normovolemic hemodilution, contrast-enhanced ultrasound, hydroxyethyl starch, renal microcirculation, sublingual microcirculation

INTRODUCTION

Acute normovolemic hemodilution (ANH) is a technique used to reduce the need for allogeneic blood transfusions in the perioperative setting. Dilutional anemia associated with ANH, however, has been identified as an important risk factor in the development of acute kidney injury (AKI) among patients undergoing cardiopulmonary bypass (1, 2). Although albumin can be used for this purpose its scarcity and costs make synthetic colloids such as hydroxyl ethyl starch (HES) and attractive alternative in the perioperative setting (3).

Recently, it has been reported that using 30 mL/kg of 6% hydroxyethyl starches (HES) 130/0.4, but not lower doses, for cardiopulmonary bypass and intraoperative fluid therapy may be associated with a greater risk of AKI (4, 5). However, the discontinuation of HES only reduced hospital length of stay but not hospital mortality rate or requirement for dialysis in a retrospective analysis of 2,170 patients with bypass surgery (6). On the other hand a recent propensity matched clinical study in surgical patients it has been shown that % 6 HES 130/0.4 was not associated with the severity and incidence of AKI and resulted in a reduction in the need for renal replacement therapy (RRT) (7). In addition a randomized controlled trial in surgical patients comparing the use of albumin to HES, found no differences with regards to renal dysfunction between the

Address reprint requests to Dr. Bülent Ergin, PhD, Department of Intensive Care, Laboratory of Translational Intensive Care, University Medical Center Rotterdam, Dr. Molewaterplein 40, 3015 GD, Rotterdam, The Netherlands. E-mail: b.ergin@erasmusmc.nl

This study was financially supported by an Innovation Grand of the Dutch Kidney Foundation (14 OI 11) and NanoNextNL, a micro- and nanotechnology consortium of the Government of the Netherlands.

Dr. Can Ince runs an Internet site microcirculationacademy.org which is part of Active Medical BV in which he holds shares, and which offers services and products related to clinical microcirculation. He has received honoraria and independent research grants from Fresenius-Kabi, Baxter Health Care, Cytosorbents and AM-Pharma; has developed SDF imaging; is listed as an inventor on related patents commercialized by MicroVision Medical under a license from the Academic Medical Center; and has been a consultant for MicroVision Medical in the past but has not been involved with this company for more than 5 years.

The remaining authors have declared no conflicts of interest.

Supplemental digital content is available for this article. Direct URL citation appears in the printed text and is provided in the HTML and PDF versions of this article on the journal's Web site (www.shockjournal.com).

DOI: 10.1097/SHK.0000000000001862

use of these two colloids (8). Even though HES is a better plasma volume expander than crystalloids and is more readily available than albumin, no information regarding the nature of intra-renal microcirculatory alterations in the kidney and whether such alterations are present in other more accessible microcirculatory beds such as the sublingual area during HES-induced ANH.

In the present study, we tested the hypotheses that;

1. HES used as a colloid in perioperative setting for inducing acute normovolemic hemodilution is effective in maintaining adequate renal microcirculatory perfusion and function down to clinically acceptable hematocrits,
2. that intrarenal microcirculatory perfusion can be measured using contrast-enhanced ultrasound (CEUS) imaging and
3. that HES-induced ANH changes in renal microcirculatory hemodynamics can be followed by hand held vital microscopy in a clinically more accessible location such as the sublingual area.

We investigated the effects of ANH to hematocrit levels beyond that used clinically to a Hct of 10% to identify levels where alterations in microcirculatory and functional parameters are apparent.

MATERIALS AND METHODS

Experiments were conducted on 15 female pigs (crossbred Landrace × Yorkshire, 3–4 months old) with permission of the local animal experimental committee (EMC3379 142-14-01) and in strict accordance with the Directive 2010/63/EU of the European Parliament and National Guidelines for Animal Care and Handling. The animals were randomly divided into two groups: with (ANH group, n = 8) or without ANH (control group, n = 7). The mean ± standard deviation (SD) body weight of the animals was 27.2 ± 1.6 kg.

Animal preparation

After overnight fasting with free access to water, all animals were premedicated with an intramuscular injection of tiletamine (5 mg/kg), zolazepam (5 mg/kg) (Zoletil, Virbac Laboratories, Carros, France) and xylazine (2.25 mg/kg) (Sedazine ® 2%, AST Farma B.V. Oudewater, the Netherlands). Intravenous access was achieved by cannulation of an ear vein; anesthesia was maintained with intravenous infusion of midazolam (1.5 mg/kg/h, Actavis, New Jersey), ketamine (5 mg/kg/h, Alfasan, Woerden, the Netherlands), and sufentanil (4 μg/kg/h, Sufenta Forte, Janssen Pharmaceuticals, Ltd., USA). Muscle relaxation was achieved with infusion of rocuronium bromide (4 mg/kg/h, Fresenius Kabi, Germany). The surgical protocol was described in a previous study (9). Briefly, all animals were intubated through a midline cervical tracheostomy using an endotracheal tube (7.0 Fr), which was placed in the trachea. Via this tube, the animal was ventilated in a pressure-controlled mode (Servo 300, Siemens-Elema, Solna, Sweden) with a fraction of inspired oxygen of 0.40, a frequency that achieves normocapnia and a positive end-expiratory pressure of 5 cm H_2O. Body temperature was monitored with a temperature probe in the nose and maintained at approximately 38–40°C with a heating pad. After establishing intravenous access of the auricular vein, anesthetics and fluid maintenance (10 mg/kg/h with balanced crystalloid) (Sterofundin® ISO, B. Braun Melsungen, Germany) were continuously infused throughout the experiment. The left femoral artery was cannulated with a 20-gauge catheter connected to a pressure transducer and used for sampling and continuous measurements of mean arterial blood pressure (MAP) and heart rate (HR). While a catheter in the right femoral artery was used for withdrawing the blood, another catheter in femoral vein was used for HES infusion in order to induce the stepwise hemodilution. After catheterization of the right external jugular vein, which was also used to administer drugs and ultrasound contrast agent, a Swan-Ganz catheter (Edwards Lifesciences, Irvine, CA) was inserted via the introducer to measure central venous pressure (CVP), mean pulmonary arterial pressure (MPAP) and thermodilution CO. A midline abdominal incision was made, and a cystostomy tube was inserted into the bladder with double purse-string sutures for the collection of urine samples. The right kidney was exposed via an incision in the right flank to evaluate renal cortical microvascular perfusion using CEUS and LSI. When all surgical procedures were completed, a perivascular ultrasonic transient time flow probe (Transonic Systems, Ithaca, NY) was placed around the right renal artery and connected to a flow meter (model T206, Transonic Systems, Elsloo, the Netherlands) for continuous measurement of renal blood flow (RBF).

Experimental protocol and hemodynamic measurements

Following the surgical procedures, a 45- to 60-minute resting period was allowed, and BL measurements were taken when the animal's hemodynamics had stabilized (MAP > 60 mm Hg and HR < 110 bpm). After BL, ANH was induced by the replacement of blood with 6% hydroxyethyl starch 130/0.4—Ringer acetate (HES-RA) (Volulyte, Fresenius Kabi, Germany) until the hematocrit value (Hct) reached 20%, 15%, and 10%. For the control animals, the time between each consecutive time point (BL, T1, T2, and T3) was ~45 minutes. Hemodynamic parameters were monitored continuously throughout the experiment. In addition to urine, arterial and venous blood samples were used for the determination of blood gas, electrolytes, and blood variables at the end of the baseline period (BL) and at each Hct target value. At these specific time points, we measured microvascular perfusion in two different tissues: renal microcirculation (measured using CEUS imaging and LSI) and sublingual microcirculation (measured using Cytocam-IDF). At the end of the experiment, the animals were euthanized with a 5 mL bolus of potassium chloride.

Global oxygenation

Arterial oxygen content (CaO_2) was calculated using the following equation: $(1.34 \times Hb \times S_aO_2) + (0.003 \times P_aO_2)$, where Hb represents hemoglobin (mmol/L), SaO_2 (%) arterial hemoglobin oxygen saturation and PaO_2 (mm Hg) arterial partial oxygen pressure. Central venous oxygen content (CvO_2) was calculated as $(1.34 \times Hb \times S_vO_2) + (0.003 \times P_vO_2)$, where SvO_2 represents mixed venous hemoglobin saturation and PvO_2 represents venous partial oxygen pressure. Global oxygen delivery was calculated as DO_2 (L/min) = $CO \times CaO_2$. Global oxygen consumption was calculated as VO_2 (L/min) = $CO \times (CaO_2 - CvO_2)$. The oxygen extraction ratio (ERO_2) was calculated as $(VO_2 / DO_2) \times 100$.

Blood gases, electrolytes, lactate, and creatinine

Arterial blood samples (0.5 mL) were taken from the femoral artery at baseline (BL) and at the three time points of Hct levels. The samples were used for determination of blood gas values, as well as for determination of the hemoglobin oxygen saturation and hemoglobin, lactate, sodium, and potassium concentrations (ABL 800 flex blood gas analyzer: Radiometer, Copenhagen, Denmark). The serum samples were used for evaluation of serum creatinine levels (Cobas 80000 c 502 Roche Diagnostic, IN).

Renal function

Creatinine clearance (C_{cr}) was measured as an index of the glomerular filtration rate and calculated with the following formula: C_{cr} (mL/min) = $(U_{crea} \times V)/P_{crea}$. Additionally, the excretion fraction of Na^+ [$EFNa^+$ (%)] was calculated and used as a marker of tubular function in the following formula: $EFNa^+ = (UNa^+ \times P_{crea})/(PNa_+ \times U_{crea}) \times 100$, where UNa^+ was the Na^+ concentration in urine and PNa^+ was the Na+ concentration in plasma. The total amount of sodium reabsorbed (TNa^+, mmol/min) was calculated according to $(C_{cr} \times PNa^+) - UNa^+ \times V$. Serum neutrophil gelatinase-associated lipocalin (NGAL) levels were measured in both the H (n = 7) and C groups (n = 5) using an enzyme-linked immunosorbent assay (ELISA) kit (KIT 044, BioPorto Diagnostic, Hellerup, Denmark).

Contrast-enhanced ultrasound imaging of the kidney

Contrast-enhanced ultrasound (CEUS) imaging using a Vevo2100 high-resolution ultrasound scanner (Fujifilm VisualSonics, Toronto, ON, Canada) was performed in the hemodilution and control groups at BL and after each Hct target was achieved (Fig. 1). At each time point, a 0.4-mL bolus of Definity® ultrasound contrast agent comprised of microbubbles with a mean diameter of 1.1 to 3.3 μm (Lantheus Medical Imaging, North Billerica, MA) was manually injected into the jugular vein followed by a 10-mL saline flush. To suppress ultrasound contrast agent-induced pseudoallergic reactions leading to pulmonary hypertension, dipyridamole (Persantine®, Boehringer Ingelheim, Alkmaar, the Netherlands) was administered at a rate of 10 μg/kg/min for 30 minutes prior to the first ultrasound contrast agent bolus at BL, and a 0.5-mL bolus of 0.8 mg/mL sildenafil (Revatio, Pfizer, New York City, NY) was administered a few minutes before each injection of ultrasound contrast agent (9–11).

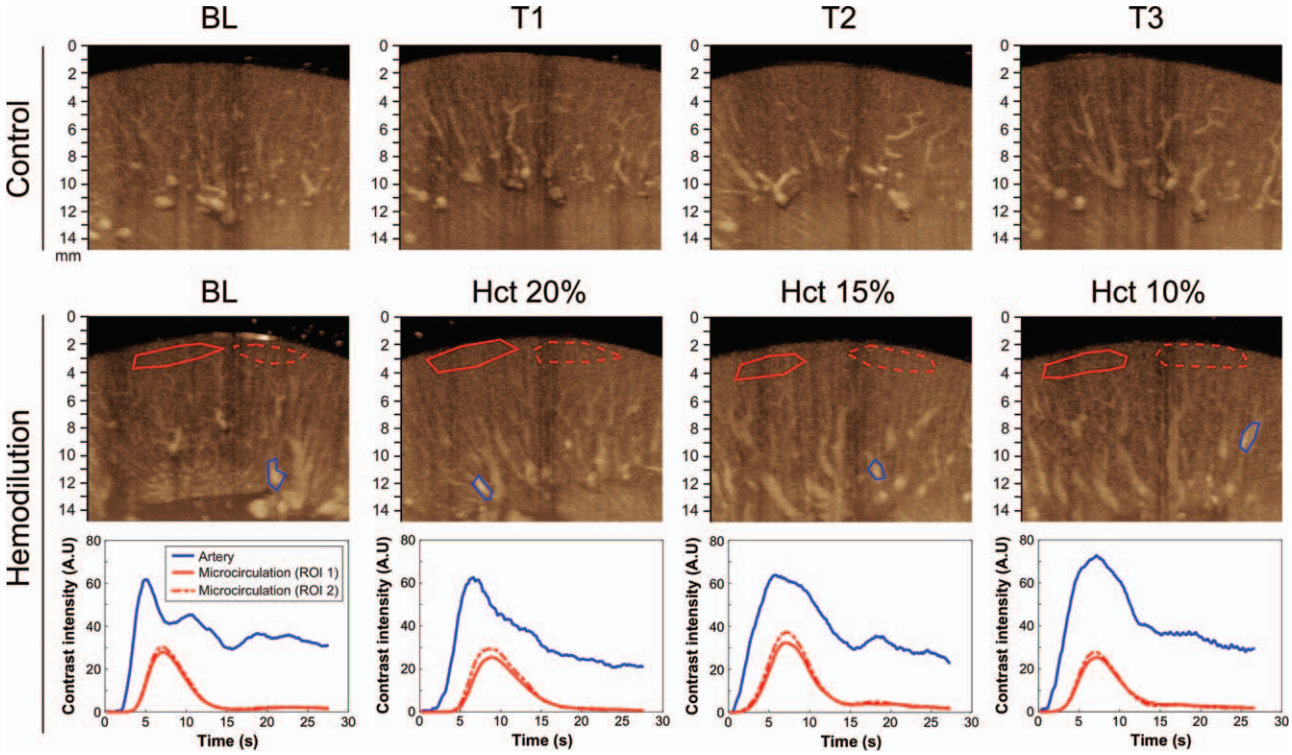

FIG. 1. **Microbubble distribution and kinetics after its injection in the kidney during BL, at Hct 20% (T1), at Hct 15% (T2) and at Hct 10% (T3).** For detection of renal microcirculatory perfusion, interlobar arteries (blue lines) and two regions of interest in the renal cortex (red solid and red dashed lines) were identified in the CEUS images and quantified in those regions of interest. AU, arbitrary units; CEUS indicates contrast-enhanced ultrasound; ROI, region of interest.

CEUS data analysis

First, correction for tissue motion in the imaging plane was applied as described elsewhere (12, 13). Three regions of interest (ROIs) were chosen for each DICOM recording: an ROI for the arteries (0.31 mm in diameter) in the deeper cortex (>8 mm depth) and two ROIs for the microcirculation in the cortex, from just below the surface of the kidney to a depth of 1.5 to 2.5 mm. The intensities of all pixels in the ROI were summed and divided by the area of the ROI for each frame, resulting in a time-intensity curve (TIC) for each ROI. Next, the semiquantitative parameters of interest were obtained from these filtered TICs: slope (SL), peak enhancement (PE), full width at half maximum (FWHM), arrival time of microbubble contrast from the injection side to the renal cortex, wash-in time (WiT), and area under the curve (AUC) during wash-in (WiAUC) (14, 15). In addition to these predefined parameters, another parameter that we previously defined as the intrarenal mean transit time (IRMTT) was assessed (9): the difference in arrival time of microbubbles in the arteries and the renal cortex ($dT_{artery} - dT_{ROIs}$), which may be used to determine the renal microvascular heterogeneity and distribution of perfusion at the different time points. No spatial differences were present in the data from two ROIs in the cortex just below the kidney surface, allowing for treating the data as one ROI. Our previous research also clearly showed that the two ROIs in the cortex were almost identical (9).

Laser speckle imaging of the kidney

LSI was used to visualize the spatiotemporal changes in renal cortical perfusion in the control group and during ANH at the BL, T1, T2, and T3 time points using the settings described in our previous work (9). Briefly, for LSI measurements, a commercially available system was used (Moor Instruments, Devon, UK), in which a near-infrared laser source operating at 785 nm illuminated the renal cortex with a penetration depth of approximately 1 mm (16).

Sublingual microcirculation

Sublingual microcirculation was measured using the Cytocam system (Braedius Medical, Naarden, the Netherlands), which is based on hand held vital microscopy, and IDF was performed only in the hemodilution group (17, 18). The microcirculatory parameters were described as total vessel density (TVD) and perfused vessel density (PVD) and red blood cell velocity (RBCv) (9). Details of the analysis can be found elsewhere (17).

Statistical analysis

Normal distributed data are expressed as the mean ± SD. Repeated measures 2-way analysis of variance (ANOVA) (2 factors: time as a related sample factor and group as an independent sample factor) with *post hoc* Sidak's and Tukey's correction tests for multiple analyses were used to determine inter- and/or intragroup differences in hemodynamic parameters, oxygenation, renal function, perfusion, biochemistry, CEUS-derived parameters, and RBC velocity. Standard one-way ANOVA with Bonferroni's correction was used for the analysis of sublingual microcirculation and NGAL. Person's correlation coefficient was used to determine the relationships among IRMTT, NGAL, and HR. Statistical analyses were performed using GraphPad Prism version 7.0a for Mac (GraphPad Software, La Jolla). A P-value < 0.05 was considered significant. G∗power software (Heinrich Heine University Dusseldorf, Germany) was used to calculate the sample size.

RESULTS

Systemic hemodynamics, electrolytes, and blood gas parameters

Data on the systemic macrohemodynamics, electrolytes, and blood gases are summarized in Table 1 and Supp. Table 1, http://links.lww.com/SHK/B365. Although MAP gradually decreased during hemodilution at Hct 15% and Hct 10% with respect to BL ($P < 0.05$), HR and CO were significantly higher at Hct 10% than at BL, Hct 20%, and Hct 15% in the hemodilution group and significantly higher than that in the control group at T3. CVP was lower in the hemodilution group at Hct 10% than in the control group at T3. SVR was decreased at Hct 10% with respect to the hemodilution group at BL, Hct 20%, Hct 15%, and with respect to the control group at T3. No

Table 1. **Systemic hemodynamics**

	BL	T1 (Hct 20%)	T2 (Hct 15%)	T3 (Hct 10%)
MAP (mm Hg)				
Control	82 ± 7	72 ± 7	68 ± 5*	66 ± 5*
Hemodilution	83 ± 11	74 ± 10	71 ± 8*	68 ± 6*
HR (BPM)				
Control	79 ± 6	86 ± 17	87 ± 14	85 ± 16
Hemodilution	80 ± 11	79 ± 7	86 ± 10	106 ± 18*,+,#,$
CVP (mm Hg)				
Control	8 ± 3	9 ± 2	8 ± 3	9 ± 2
Hemodilution	6 ± 2	6 ± 2	7 ± 1	6 ± 1$
CO (L/min)				
Control	3.7 ± 0.5	3.5 ± 0.5	3.5 ± 0.5	3.5 ± 0.4
Hemodilution	4.1 ± 0.6	3.9 ± 0.6	4.6 ± 0.9$	6.7 ± 1.1*,+,#,$
MPAP (mm Hg)				
Control	18 ± 2	20 ± 2$	21 ± 3	21 ± 4
Hemodilution	17 ± 3	16 ± 3	17 ± 2	18 ± 2
SVR (dynes.s.cm^{-5})				
Control	1630 ± 159	1425 ± 416	1287 ± 213	1319 ± 371
Hemodilution	1509 ± 330	1383 ± 262	1104 ± 314*	704 ± 128*,+,#,$

CO indicates cardiac output; CVP, central venous pressure; HR, heart rate; MAP, mean arterial pressure; MPAP, mean pulmonary arterial pressure; SVR, systemic vascular resistance. Values are presented as the mean ± SD.
*$P < 0.05$ vs. BL.
+$P < 0.05$ vs. T1.
#$P < 0.05$ vs. T2.
$$P < 0.05$ vs. the control group at the same time point.

significant differences were observed in the plasma Na^+, K^+, pH, $etCO_2$, PaO_2, and SvO_2 values. However, low base excess was observed in the hemodilution group at Hct 10% compared to BL and Hct 20% and with respect to the control group at T3.

Global oxygen delivery and consumption

Data on global oxygen delivery and consumption and lactate levels are summarized in Table 2. CaO_2 gradually and significantly decreased over time in the hemodilution group at Hct 20%, 15%, and 10% and significantly differed from that in the control group at the same time points, for example, T1, T2, and T3, respectively ($P < 0.05$). CvO_2 significantly decreased from BL to Hct 15% and Hct 10% and was also significantly lower than that in the control group at the same time points ($P < 0.05$). Despite systemic DO_2 and VO_2 being marginally depleted, ERO_2 and plasma lactate were stable in

Table 2. **Systemic perfusion variables**

	BL	T1 (Hct 20%)	T2 (Hct 15%)	T3 (Hct1 0%)
CaO_2 (mL/dL)				
Control	6.26 ± 0.58	6.57 ± 0.68	6.59 ± 0.64	6.57 ± 0.33
Hemodilution	6.18 ± 0.41	5.25 ± 0.28*,$	4.22 ± 0.47*,+,$	3 ± 0.3*,+,#,$
CvO_2 (mL/dL)				
Control	4.01 ± 0.8	3.98 ± 0.77	3.93 ± 0.69	4.05 ± 0.61
Hemodilution	3.82 ± 0.70	3.18 ± 0.49	2.48 ± 0.58*,$	1.74 ± 0.36*,+,$
DO_2 (mL/min)				
Control	23.73 ± 4.85	23.17 ± 3.73	23.38 ± 3.72	23.44 ± 3.55
Hemodilution	25.70 ± 5.19	20.40 ± 3.40	19.70 ± 4.64*	20.28 ± 5
VO_2 (mL/min)				
Control	8.35 ± 1.72	9.20 ± 1.75	9.35 ± 1.45	9.10 ± 2.37
Hemodilution	9.69 ± 1.43	8.15 ± 1.86	7.98 ± 1.37	8.42 ± 2.18
ERO_2 (%O_2)				
Control	36 ± 9	40 ± 6	41 ± 7	39 ± 8
Hemodilution	39 ± 8	40 ± 7	42 ± 9	42 ± 8
Lactate (mmol/L)				
Control	1.5 ± 0.2	1.5 ± 0.9	0.9 ± 0.1	1.0 ± 0.2
Hemodilution	1.1 ± 0.3	1.1 ± 0.4	0.9 ± 0.3	0.9 ± 0.4

CaO_2 indicates arterial oxygen content; CvO_2, venous oxygen content; DO_2, oxygen delivery; ERO_2, O_2 extraction ratio; VO_2, oxygen consumption. Values are presented as the mean ± SD.
*$P < 0.05$ vs. BL.
+$P < 0.05$ vs. T1.
#$P < 0.05$ vs. T2.
$$P < 0.05$ vs. the control group at the same time point.

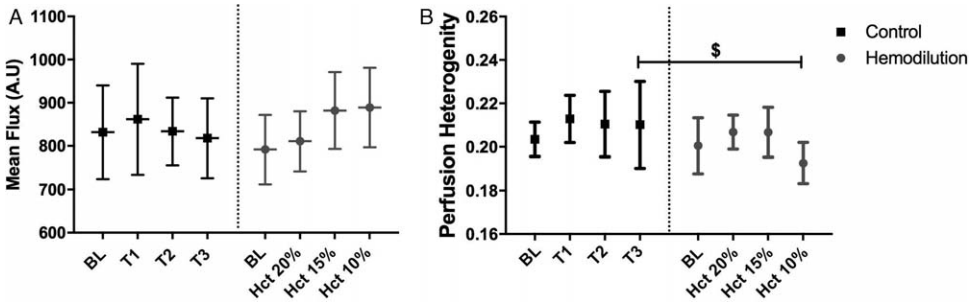

Fig. 2. **Renal microvascular perfusion (panel A) and perfusion heterogeneity (panel B).** Values are presented as the mean ± SD, $^{\$}P < 0.05$ vs. the control group at the same time points.

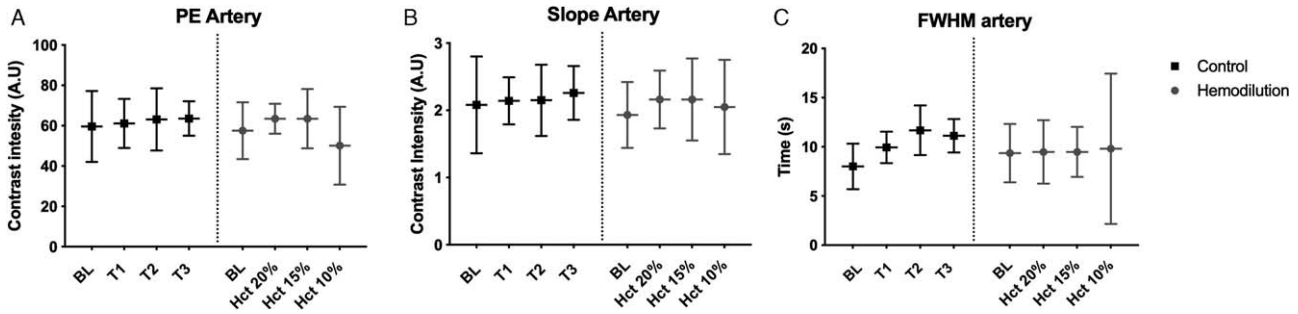

Fig. 3. **Results of the contrast-enhanced ultrasound analysis in the interlobar arteries.** For (A) SL artery; (B) PE, and (C) FWHM. Values are presented as the mean ± SD. FWHM indicates full width half maximum; PE, peak enhancement; SL, slope.

both the control and hemodilution groups throughout the experiments.

Renal cortical microvascular perfusion

The mean cortical perfusion and perfusion heterogeneity values are presented in Figure 2. Perfusion heterogeneity was significantly lower at Hct 10% than in the control group at T3 ($P < 0.05$), while the mean perfusion values did not significantly change throughout the hemodilution process.

CEUS parameters

All data obtained from the CEUS measurements are presented in Figures 3 and 4. In the interlobar renal arteries, SL, PE, and FWHM remained constant during the ANH procedure

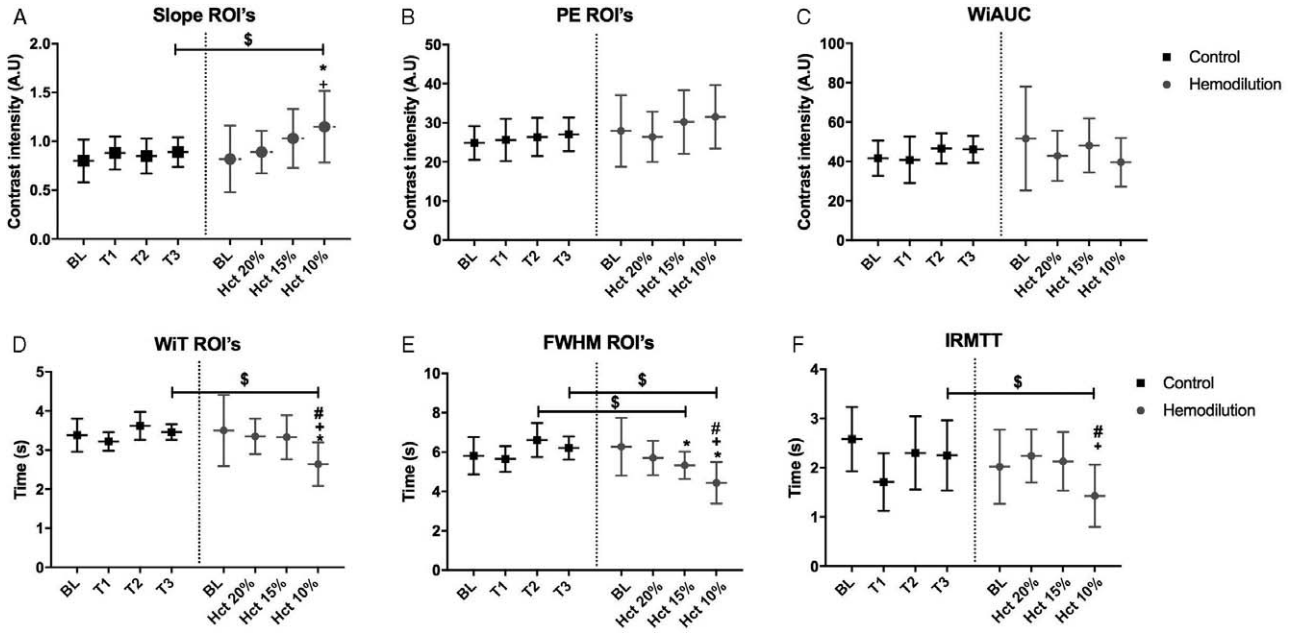

Fig. 4. **Results of the contrast-enhanced ultrasound analysis in the microcirculation of the renal cortex.** (A) slope (SL); (B) peak enhancement (PE); (C) area under the wash-in curve (WiAUC); (D) wash in time (WiT); (E) full-width half maximum (FWHM), and (F) intrarenal mean transit time (IRMTT). Values are presented as the mean ± SD, $^{*}P < 0.05$ vs. BL, $^{+}P < 0.05$ vs. Hct 20% (T1), $^{\#}P < 0.05$ vs. Hct 15% (T2), and $^{\$}P < 0.05$ vs. the control group at the same time points. FWHM indicates full width half maximum; IRMTT, intrarenal mean transit time; PE, peak enhancement; SL, slope; WiAUC, area under the wash-in curve; WiT, wash in time.

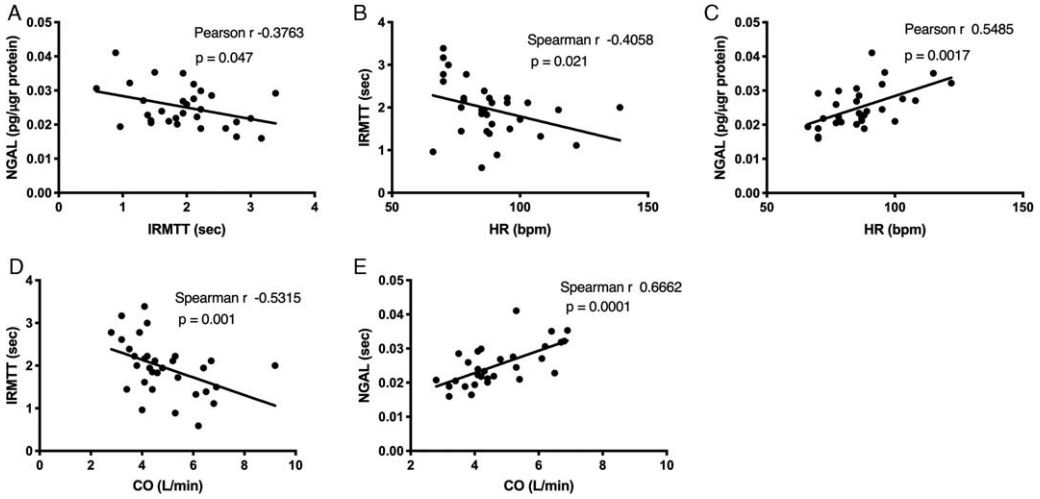

Fig. 5. **Correlations among the IRMTT, HR, and plasma NGAL levels, $P < 0.05$.** HR indicates heart rate; IRMTT, intrarenal mean transit time; NGAL, neutrophil gelatinase-associated lipocalin.

(Fig. 3). However, in the renal cortex, SL was steeper in the hemodilution group at Hct 10% than at BL, indicating a faster inflow of microbubbles, consistent with the finding that FWHM that was significantly lower at Hct 10% than at BL ($P < 0.05$). At Hct 10%, FWMH was also significantly lower than at Hct 20% and Hct 15% ($P < 0.05$). In addition, FWHM was significantly lower at Hct 15% and Hct 10% in the hemodilution group than in the control group at T2 and T3 ($P < 0.05$), respectively. The WiT significantly decreased, also indicating faster inflow, at Hct 10% with respect to the other time points of the hemodilution group, as well as with the control groups at T3 ($P < 0.05$). The constant PE and WiAUC throughout the hemodilution process suggest that the concentration of microbubbles flowing through the kidney after every bolus injection remained constant. The IRMTT, the difference in arrival time of microbubbles between the renal small arteries and the microcirculation in the renal cortex, was significantly lower at Hct 10% in the hemodilution group than at T3 in the control group ($P < 0.05$), also indicating an increase in blood velocity ($P < 0.05$) (Fig. 4). In addition, the IRMTT was negatively correlated with HR ($r = 0.3548$, $P = 0.0463$) (Fig. 5).

Sublingual microcirculation

No significant microcirculatory alterations were found in TVD and PVD throughout the hemodilution process (Fig. 6). However, the RBC velocity in the sublingual area was significantly elevated at Hct 20%, 15%, and 10% (Fig. 7).

Renal function and injury

Renal blood flow (RBF), plasma urea, urine output, and urine osmolality values are summarized in Table 3. RBF and urine output were significantly higher in the hemodilution group at Hct 10% than in the control group at T3 ($P < 0.05$). Additionally, urine osmolality was significantly lower in the hemodilution group at Hct 10% than in the control group at T3 ($P < 0.05$). Renal functional parameters are represented in Figure 8. Although creatinine clearance, TNa^+ and $EFNa^+$ were stable through the hemodilution process (Fig. 8A–C), the serum NGAL levels were higher at Hct 15% and Hct 10% than at BL, and the NGAL concentration at Hct 10% was significantly higher than that in the control group at T3 ($P < 0.05$) (Fig. 8D). There was also a negative correlation between NGAL levels and IRMTT ($r = -0.3763$, $P = 0.047$) and a

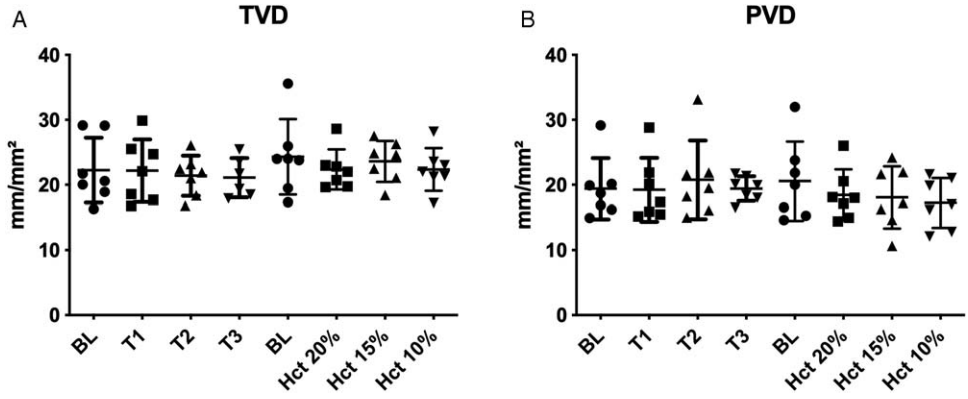

Fig. 6. **Sublingual microcirculatory parameters.** (A) TVD; (B) PVD. Values are presented as the mean ± SD. PVD indicates perfused vessel density; TVD, Total vessel density.

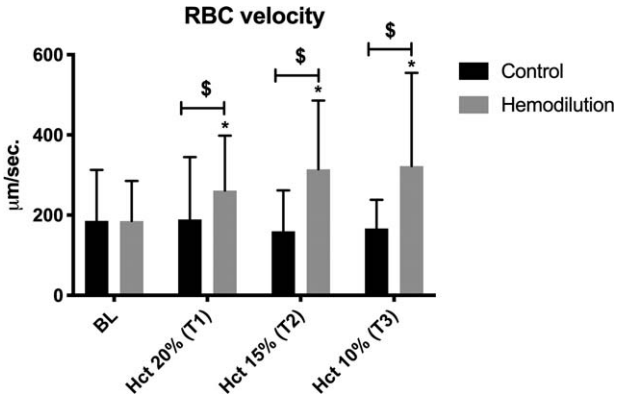

Fig. 7. **Results of RBC velocity in the sublingual area.** Values are presented as the mean ± SD, $^{*}P < 0.05$ vs. BL, $^{\$}P < 0.05$ vs. the control group at the same time points.

positive correlation between NGAL and HR ($r = 0.5485$, $P = 0.0017$) (Fig. 5).

DISCUSSION

In the present study, we found that

1. HES-induced ANH was associated with a sustained renal microcirculatory perfusion which could be successfully assessed by CEUS with maintained systemic hemodynamic and oxygenation parameters
2. that HES induced ANH at clinically acceptable levels of Hct (>15%) did not cause renal dysfunction and injury, and
3. that microcirculatory alterations such as RBC velocity observed in the kidney using CEUS and LSI parallel those measured sublingually measured using hand-held vital microscopy.

In this study, we confirmed in a pig model that hemodilution in the range used clinically (>15%) could maintain hemodynamic and oxygenation parameters such as MAP, HR, CO, DO_2, and ERO_2. Similar findings have been reported by Konrad et al., who showed that compared to colloids, where HES was used as the colloid, crystalloids led to more perturbations of systemic hemodynamics, renal microvascular oxygenation and function in pigs than did HES (19). Importantly, in our previous study, we had demonstrated a divergent effect between the macro- and microcirculation as well as between sublingual (measured by HVM) and intrarenal microcirculation (measured by CEUS) in resuscitated pigs with septic shock (9). In contrast our present study showed that such a divergence between macro- and microcirculatory did not exist in ANH and that instead there was a coherence between the macro- and microcirculation, which suggests that systemic hemodynamic variables (CO and HR) can support the microcirculation (sublingual), maintain adequate oxygen supply to the parenchymal cells (RBF) and sustain organ function (lactate, urine output, and C_{cr}).

In the sublingual microcirculation, we did not observe any prominent changes in the perfused vessel density (or changes in TVD) following titration of red blood cells with HES solution. This result might be explained by the fact that the colloidal solution can preserve the intravascular volume and perfusion in peripheral tissues. Similarly, Funk et al. showed that in contrast to Ringer lactate, colloid solution (dextran) did not cause any significant alteration of systemic hemodynamics, capillary flow velocity, or functional capillary density in isovolemic hemodilution model of hamsters (20).

The kidney is one of the most sensitive organs to hemodynamic instability and hypoxia due to the complexity of the renal microvasculature, functional discrepancy of different regions, and workload (1/4 of CO) (21). Konrad et al. demonstrated that ANH with HES preserved renal cortical and inner medullar oxygenation compared to hemodilution using crystalloids at Hct 15% (19). Despite the fact that we do not have specific renal oxygenation results, we showed that ANH with HES is accompanied by

1. an increase in renal blood flow,
2. an increase in intrarenal blood velocity, and
3. high urine output during the hemodilution process.

Moreover, even if systemic vascular resistance is low, high urine output shows efferent arteriolar vasoconstriction as a

Table 3. **Results of RBF, plasma urea, urine output and urine osmolality**

	BL	T1 (Hct 20%)	T2 (Hct 15%)	T3 (Hct 10%)
RBF (mL/min)				
Control	261 ± 52	218 ± 27	218 ± 24	209 ± 36
Hemodilution	255 ± 55	255 ± 70	272 ± 31	289 ± 46$^{\$}$
Urea (mmol/L)				
Control	2.3 ± 0.4	2.9 ± 0.9	3.2 ± 0.8	3.4 ± 0.8
Hemodilution	2.6 ± 0.4	2.9 ± 0.6	3.1 ± 0.7	3.2 ± 0.8
Urine output (mL/h)				
Control	22 ± 37	13 ± 4	13 ± 4	12 ± 5
Hemodilution	26 ± 13	22 ± 12	23 ± 8	27 ± 9$^{\$}$
Urine osmolality (mOsm/kg H_2O)				
Control	643 ± 136	753 ± 148	772 ± 177	806 ± 183
Hemodilution	572 ± 135	692 ± 192	697 ± 172	585 ± 92$^{\$}$

C_{Cr}, creatinine clearance; RBF, renal blood flow. Values are presented as the mean ± SD.
$^{\$}P < 0.05$ vs. the control group at the same time points.

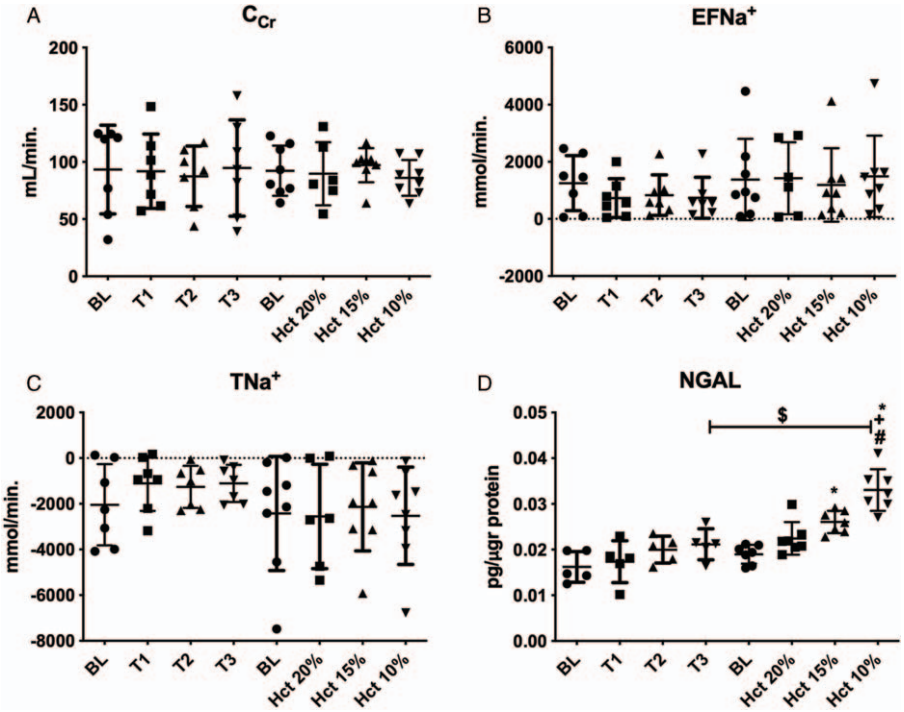

Fig. 8. **Renal functional parameters and serum NGAL levels between the control and hemodilution groups.** (A) C_{cr}; (B) $EFNa^+$; (C) TNa^+; (D) (NGAL). Values are presented as the mean ± SD, $^*P < 0.05$ vs. BL, $^+ < 0.05$ vs. Hct 20%, $^\#P < 0.05$ vs. Hct 15%, and $^\$P < 0.05$ vs. the control group at the same time points. C_{cr}, Creatinine clearance; $EFNa^+$, fractional sodium extraction; NGAL, neutrophil gelatinase-associated lipocalin; TNa^+, tubular sodium reabsorption.

result of renal autoregulation. A study conducted by Ghatanatti et al. in cardiopulmonary bypass patients demonstrated that although Hct < 21% correlated with a greater risk of AKI than Hct > 21% due to a significant reduction of the glomerular filtration rate (GFR) and C_{Cr}, only 4% of patients required dialysis (22). However, in our study on pigs, we did not find a reduced C_{cr}, even though Hct was decreased to 10%. In accordance with the KDIGO plasma creatinine criteria (23), HES-RA resuscitation did not cause AKI as a short-term effect of ANH, but the result of plasma NGAL levels clearly indicated renal damage following ANH. However, similar to colloids, crystalloids can also cause renal damage in perioperative settings. Konrad et al., demonstrated that ANH with crystalloid is associated with higher renal tissue edema and expression of hypoxia-inducible factor-1α (HIF-1 α) in comparison to colloid (19). Additionally, Baranauskas et al. showed that postoperative AKI measured by NGAL after cardiac surgery was directly correlated with perioperative hemodilutional anemia mediated by crystalloid priming solution (24). Briefly, we found that regardless of using a colloid, ANH was associated with renal injury, as shown by a gradual increase in serum NGAL levels despite preserved renal function, although this effect was found to be statistically significant only at a Hct of 10%. Another important finding in this study is that alteration of serum NGAL levels during the hemodilution process was correlated with CO. Thus, CO and HR seem to be important parameters possibly related to renal damage during perioperative fluid management.

Although LSI showed no alteration of renal cortical microvascular perfusion, the perfusion heterogeneity tended to decrease during hemodilution, indicating that all parts of the kidney are homogenously perfused. In addition to the sublingual microcirculatory results, CEUS results also showed unaltered PE and WiAUC, which indicated that the intrarenal blood volume was sustained by HES-RA even at the lowest Hct levels. Interestingly, FWHM, PE, and SL also showed that both blood velocity and blood volume were not altered in the renal artery, probably because vasoconstriction does not play a significant role in the renal artery. In contrast to the renal artery, both CEUS imaging and sublingual assessments showed a progressive increment of RBC velocity in the sublingual area and in the kidney (increase in SL, combined with a decrease in FWHM, WiT, and IRMTT). In parallel, high flow velocity as measured by the FWHM indicates a reduced arrival time of contrast from the jugular injection to the renal cortex. Thus, to distinguish the effect of systemic and renal alterations on blood velocity, we used IRMTT as an indicator of macro- to microcirculatory flow transition ($dT_{artery} - dT_{ROIs}$). This showed a substantially higher intrarenal blood flow velocity, confirming the presence of intrarenal vascular autoregulation. This autoregulation is associated with efferent arteriolar vasoconstriction, which results in an increased intraglomerular pressure, higher glomerular filtration rate, and higher urine output. Importantly, high intra renal velocity might be a specific cause of renal hypoxia and damage due to diminished oxygen extraction affected by the short transit times of RBCs. Hence, Presson et al. measured the entire transit time distribution for RBCs crossing single subpleural capillary networks in canine lungs using *in vivo* fluorescence video microscopy and concluded that a decrease in transit times of RBCs or high CO also impaired the complete saturation of red blood cells (25). In the present

study, we also proved that high CO and HR are correlated with a decreased intrarenal transit time of RBCs. In addition, Jespersen and Østergaard found that oxygen extraction was more impaired when mean transit times decreased, in combination with a heterogeneous increase in flow velocities (26). In addition to the studies mentioned the high RBC velocity perturbed oxygen release from RBCs, we also observed high intrarenal RBC velocity and its association with renal damage during hemodilution. Therefore, it should be noted that a long exposure to high intrarenal RBC velocity might impair oxygen extraction and renal function, leading to AKI; the latter was shown by the preexistence of renal damage with increased NGAL. However, the reduced oxygen carrying capacity of blood caused by ANH-induced dilutional anemia could also underly this effect. We also showed that alteration of sublingual microcirculatory perfusion was reflected by parallel changes of the intrarenal perfusion pattern. In contrast to our previous study on sepsis in pigs (9), in the present study, we did not detect any plugged vessels or slow flow as a possible cause of HES-related coagulopathy in either the sublingual or renal microcirculation.

To conclude, we demonstrated that ANH with HES-RA maintained systemic and renal hemodynamics, as well as microcirculation and renal function. We also showed that the reduced oxygen-carrying capacity of blood by using HES under certain conditions (Hct 10%) might not impair systemic oxygenation and renal function because it promotes adequate expansion of plasma volume to maintain oxygen delivery and cardiac output in the short term of hemodilution. In the kidney, despite that ANH itself can induce tissue hypoxia due to the low oxygen carry capacity of blood (especially at a Hct of 10%), we found that high intrarenal blood velocity at low Hct and viscosity could contribute to renal injury following ANH. Therefore, we conclude that

1. HES induced ANH can preserves renal function and perfusion when used at clinically acceptable levels of Hct (>15%) but can cause dilutional anemia due to intravascular volume expansion. In addition to dilutional anemia, high intra renal RBC velocity might be another factor leading to hypoxia-related renal injury at longer durations of ANH induced anemic conditions
2. that alterations of HR or CO and IRMTT assessed by CEUS may indicate impending renal injury, and
3. that noninvasive sublingual microcirculatory imaging can be used for assessing the volume status (capillary hematocrit) as and together with RBC velocity can be used for estimating possible renal injury mediated by hemodilutional anemia.

Limitations

This study has some limitations which should be considered for further studies:

1. the duration of hemodilution at Hct 10% was too short to assess the long-term effects of hemodilution on systemic hemodynamics and renal function,
2. no histological assessment of the kidney was performed to show possible tubular and glomerular damage, and
3. no crystalloid group was used.

REFERENCES

1. Habib RH, Zacharias A, Schwann TA, Riordan CJ, Engoren M, Durham SJ, Shah A: Role of hemodilutional anemia and transfusion during cardiopulmonary bypass in renal injury after coronary revascularization: implications on operative outcome. *Crit Care Med* 33(8):1749–1756, 2005.
2. Karkouti K, Beattie WS, Wijeysundera DN, Rao V, Chan C, Dattilo KM, Djaiani G, Ivanov J, Karski J, David TE: Hemodilution during cardiopulmonary bypass is an independent risk factor for acute renal failure in adult cardiac surgery. *J Thorac Cardiovasc Surg* 129(2):391–400, 2005.
3. Joosten A, Coeckelenbergh S, Alexander B, Delaporte A, Cannesson M, Duranteau J, Saugel B, Vincent J-L, Van der Linden P: Hydroxyethyl starch for perioperative goal-directed fluid therapy in 2020: a narrative review. *BMC Anesthesiol* 20(1):209, 2020.
4. Lagny M-G, Roediger L, Koch J-N, Dubois F, Senard M, Donneau A-F, Hubert MB, Hans GA: Hydroxyethyl starch 130/0.4 and the risk of acute kidney injury after cardiopulmonary bypass: a single-center retrospective study. *J Cardiothorac Vasc Anesth* 30(4):869–875, 2016.
5. Momeni M, Nkoy Ena L, Van Dyck M, Matta A, Kahn D, Thiry D, Grégoire A, Watremez C: The dose of hydroxyethyl starch 6% 130/0.4 for fluid therapy and the incidence of acute kidney injury after cardiac surgery: A retrospective matched study. *PLoS ONE* 12(10):e0186403, 2017.
6. Hong M, Jones PM, Martin J, Kiaii B, Arellano R, Cheng D, John-Baptiste AA: Clinical impact of disinvestment in hydroxyethyl starch for patients undergoing coronary artery bypass surgery: a retrospective observational study. *Can J Anaesth* 66(1):25–35, 2019.
7. Miyao H, Kotake Y: Renal morbidity of 6% hydroxyethyl starch 130/0.4 in 9000 propensity score matched pairs of surgical patients. *Anesth Analg* 130(6):1618–1627, 2020.
8. Kammerer T, Brettner F, Hilferink S, Hulde N, Klug F, Pagel J-I, Karl A, Crispin A, Hofmann-Kiefer K, Conzen P, et al.: No differences in renal function between balanced 6% hydroxyethyl starch (130/0.4) and 5% albumin for volume replacement therapy in patients undergoing cystectomy: a randomized controlled trial. *Anesthesiology* 128(1):67–78, 2018.
9. Lima A, van Rooij T, Ergin B, Sorelli M, Ince Y, Specht PAC, Mik EG, Bocchi L, Kooiman K, de Jong N, et al.: Dynamic contrast-enhanced ultrasound identifies microcirculatory alterations in sepsis-induced acute kidney injury. *Crit Care Med* 46(8):1284–1292, 2018.
10. Szebeni J, Baranyi L, Savay S, Bodo M, Morse DS, Basta M, Stahl GL, Bünger R, Alving CR: Liposome-induced pulmonary hypertension: properties and mechanism of a complement-mediated pseudoallergic reaction. *Am J Physiol Heart Circ Physiol* 279(3):H1319–1328, 2000.
11. Ostensen J, Hede R, Myreng Y, Ege T, Holtz E: Intravenous injection of Albunex microspheres causes thromboxane mediated pulmonary hypertension in pigs, but not in monkeys or rabbits. *Acta Physiol Scand* 144(3):307–315, 1992.
12. Daeichin V, Akkus Z, Skachkov I, Kooiman K, Needles A, Sluimer J, Janssen B, Daemen MJAP, van der Steen AFW, de Jong N, et al.: Quantification of bound microbubbles in ultrasound molecular imaging. *IEEE Trans Ultrason Ferroelectr Freq Control* 62(6):1190–1200, 2015.
13. Hoogi A, Akkus Z, van den Oord SCH, ten Kate GL, Schinkel AFL, Bosch JG, de Jong N, Adam D, van der Steen AFW: Quantitative analysis of ultrasound contrast flow behavior in carotid plaque neovasculature. *Ultrasound Med Biol* 38(12):2072–2083, 2012.
14. Dietrich CF, Averkiou MA, Correas J-M, Lassau N, Leen E, Piscaglia F: An EFSUMB introduction into Dynamic Contrast-Enhanced Ultrasound (DCE-US) for quantification of tumour perfusion. *Ultraschall Med* 33(4):344–351, 2012.
15. Needles A, Arditi M, Rognin NG, Mehi J, Coulthard T, Bilan-Tracey C, Gaud E, Frinking P, Hirson D, Foster FS: Nonlinear contrast imaging with an array-based micro-ultrasound system. *Ultrasound Med Biol* 36(12):2097–2106, 2010.
16. Draijer M, Hondebrink E, van Leeuwen T, Steenbergen W: Review of laser speckle contrast techniques for visualizing tissue perfusion. *Lasers Med Sci* 24(4):639–651, 2009.
17. Sorelli M, Bocchi L, Ince C: Monitoring the microcirculation at the bedside using hand-held imaging microscopes: Automatic tracking of erythrocytes. *Conf Proc IEEE Eng Med Biol Soc* 2015:7378–7381, 2015.
18. Massey MJ, Larochelle E, Najarro G, Karmacharla A, Arnold R, Trzeciak S, Angus DC, Shapiro NI: The microcirculation image quality score: development and preliminary evaluation of a proposed approach to grading quality of image acquisition for bedside videomicroscopy. *J Crit Care* 28(6):913–917, 2013.

19. Konrad FM, Mik EG, Bodmer SIA, Ates NB, Willems HFEM, Klingel K, de Geus HRH, Stolker RJ, Johannes T: Acute normovolemic hemodilution in the pig is associated with renal tissue edema, impaired renal microvascular oxygenation, and functional loss. *Anesthesiology* 119(2):256–269, 2013.
20. Funk W, Baldinger V: Microcirculatory perfusion during volume therapy. A comparative study using crystalloid or colloid in awake animals. *Anesthesiology* 82(4):975–982, 1995.
21. Ergin B, Kapucu A, Demirci-Tansel C, Ince C: The renal microcirculation in sepsis. *Nephrol Dial Transplant* 30(2):169–177, 2015.
22. Ghatanatti R, Teli A, Narayan P, Roy Chowdhuri K, Mondal A, Bhattacharya S, Sengupta G, Datta M: Ideal hematocrit to minimize renal injury on cardiopulmonary bypass. *Innovations (Phila)* 10(6):420–424, 2015.
23. Lameire NH, Levin A, Kellum JA, Cheung M, Jadoul M, Winkelmayer WC, Stevens PE, Conference Participants. Harmonizing acute and chronic kidney disease definition and classification: report of a Kidney Disease: Improving Global Outcomes (KDIGO) Consensus Conference. *Kidney Int* 100(3):516–526, 2021.
24. Baranauskas T, Kaunienė A, Švagždienė M, Širvinskas E, Lenkutis T: The correlation of post-operative acute kidney injury and perioperative anaemia in patients undergoing cardiac surgery with cardiopulmonary bypass. *Acta Med Litu* 26(1):79–86, 2019.
25. Presson RG, Graham JA, Hanger CC, Godbey PS, Gebb SA, Sidner RA, Glenny RW, Wagner WW: Distribution of pulmonary capillary red blood cell transit times. *J Appl Physiol* 79(2):382–388, 1995.
26. Jespersen SN, Østergaard L: The roles of cerebral blood flow, capillary transit time heterogeneity, and oxygen tension in brain oxygenation and metabolism. *J Cereb Blood Flow Metab* 32(2):264–277, 2012.